TiO_x–VO_x Mixed Oxides on SBA-15 Support Prepared by the Designed Dispersion of Acetylacetonate Complexes: Spectroscopic Study of the Reaction Mechanisms

Y. Segura,* P. Cool, P. Van Der Voort, F. Mees, V. Meynen, and E. F. Vansant

Department of Chemistry, Laboratory of Adsorption and Catalysis, University of Antwerp (UIA), Universiteitsplein 1, B-2610 Wilrijk, Belgium

Received: August 1, 2003; In Final Form: December 6, 2003

TiO_x−VO_x mixed oxides supported SBA-15 catalysts were prepared in a very controlled way by the designed dispersion method (MDD) using acetylacetonate complexes. The Ti and V active centers are generated by the MDD of the $TiO(acac)_2$ and $VO(acac)_2$. The process consists of the adsorption and subsequent thermolysis of the Ti−V complexes. A careful selection of synthesis conditions allows us to modify the mutual interaction of the Ti and V centers and the interaction of the active centers with the silica support. The decomposition of the anchored complexes and the conversion of the physisorbed species toward covalently bonded TiO_x−VO_x surface groups have been studied by using a home-built in-situ IR transmission cell. IR seems to be the most suitable technique to follow the calcination process that is required to understand the reaction mechanism. During the thermal conversion, the Ti−V/acac precursor is converted toward supported mixed oxide. Additional characterization was done by FTIR−PAS, TGA, chemical analysis, as well as XRD, FT-Raman, and N_2 adsorption measurements.

Introduction

The new generations of catalysts consist of a variety of active sites, yielding additional synergic effects and a support material with very specific characteristics in terms of surface area, porosity, and accessibility.[1,2] Such materials are no longer prepared by the simple conventional methods (like impregnation),[3,4,5] but are the result of the molecular designed dispersion (MDD)[6,7,8] of the active elements on carefully prepared micelle templated structures (MTS).[9]

Materials containing Ti, V, and W are known as excellent catalysts in several reduction−oxidation reactions, of which the selective catalytic reduction (SCR) of NO_x is probably the most studied process because of its great importance in the environmental research field as a demand of avoiding harmful products emitted by combustion.[10,11]

Following the MDD process, metal acac complexes are reacted with the surface hydroxyls of the support material and converted into the metal oxide form after calcination. A great variety of acac complexes on different supports have already been studied and reported in the literature,[8,12,13] getting to the conclusion that the reactivity of the support and the difference in geometry and stability of the acac ligands result in a different reaction mechanism and surface dispersion.

In particular, $VO(acac)_2$ and $TiO(acac)_2$ have also been studied separately and deposited on different supports such as silica,[14] alumina,[15] MCM-48,[16,17] or zirconia.[8]

A new type of material, which is very interesting as support in the MDD process, is the hexagonal SBA-15.[19] SBA-15 is characterized by very high pore volumes, thick pore walls, and intrinsically combined micro- and mesopores with a high surface area. Because of the controlled pore size and a very narrow pore size distribution, the ordered mesoporous materials have a large potential as catalytic support.

In this study, we present several methods to prepare titania−vanadia−SBA-15 catalysts in a controlled way. This type of catalyst combines the interesting porosity properties of the SBA-15 as a support, the chemical activity of the titania, and the properties of vanadia as a catalyst for a great variety of oxidation reactions.

A detailed characterization of catalyst precursors (before calcination) will be performed using IR transmission spectroscopy to establish the reaction mechanism of V and Ti with the silica surface. Complementary characterization is obtained by FTIR−PAS, TGA, chemical analysis, XRD, FT-Raman, and N_2 adsorption measurements for both precursors and final titania−vanadia−SBA-15 catalysts.

Experimental Section

Sample Preparation and Treatment. *1. Support.* SBA-15 was prepared by using 4 g of Plutonic P123 triblock copolymer surfactant (EO_{20}–PO_{70}−EO_{20}) dissolved in water/HCl 2 M solution. Subsequently, an amount of TEOS (tetraethyl orthosilicate) was added. The resulting mixture was stirred for 8 h at 45 °C and then aged for 15 h at 80 °C. The white product was filtered, washed, and dried. The sample was subsequently calcined at 550 °C with a heating rate of 1 °C/min and an isothermal period of 6 h in air atmosphere.

2. Metal Deposition. Single depositions of the metals on the ordered mesoporous material SBA-15 were done by the MDD method of the acetylacetonate complexes, as well as the mixed oxide deposition of the two metals on the SBA-15 support.

Deposition of the metal acetylacetonate complex ($TiO(acac)_2$ and/or $VO(acac)_2$) onto the SBA-15 surface was performed by the liquid phase designed dispersion method. A calculated amount of Ti−$VO(acac)_2$ was dissolved in 100 mL zeolite dried toluene. The dried SBA-15 was added and the solution was stirred for 1 h. After reaction, the modified support was filtered off, washed a few times with toluene, and dried under vacuum.

* Corresponding author. E-mail: segura@uia.ua.ac.be.

10.1021/jp036259w CCC: $27.50
Published on Web 02/28/2004

The reaction was carried out at RT and in absence of air. The adsorbed complex is called the precursor. The acac ligands were removed by calcination, which was performed in a programmable oven at 550 °C in air.

Two different paths to achieve the final mixed oxide catalyst were followed:

- "Route A" deposition in which V-acac was deposited on TiO_x/SBA-15 calcined. A calculated amount of $TiO(acac)_2$ was deposited on the SBA-15 by MDD. The precursor obtained was calcined at 550 °C. After that, an estimated amount of $VO(acac)_2$ was deposited on the TiO_x−SBA-15 support, filtered, washed off, dried in vacuum, and calcined at 550 °C. Deposition was carried out at RT.
- "Route B" deposition in which V-acac was deposited on Ti-acac/SBA-15 precursor.

A calculated amount of $TiO(acac)_2$ was deposited on the SBA-15 by MDD. The precursor obtained was outgassed under vacuum conditions overnight. An estimated amount of $VO(acac)_2$ was then deposited on Ti-acac/SBA-15 surface, also by liquid phase. The sample obtained was filtered, washed off, dried under vacuum, and calcined at 550 °C to create the supported titanium−vanadium mixed oxide. Deposition was carried out at RT. For both depositions, the calculated concentrations of $TiO(acac)_2$ and $VO(acac)_2$ are the same.

Characterization Methods

The concentration of the metals on the support was determined by ultraviolet and visible (UV−vis) spectrophotometry after destruction of the samples and measured colorimetrically. The measurements were performed on a Unicam 8700 UV−VIS.

For the single deposition, the samples were stirred for 20 min in hot sulfuric acid (2.5 M). After filtration H_2O_2 was added, and vanadium/titanium concentration was measured at 450 nm and at 407 nm, respectively.

For the mixed oxide deposition, the signals of both complexes are too close and they interfere. HF prevents the formation of a color-Ti^{4+} complex, therefore the concentrations of both metals can be analyzed separately, in the same way as in the single deposition.[19]

Fourier transform infrared photoacoustic spectra (FTIR−PAS) were recorded on a Nicolet 20 SX spectrometer, equipped with a McClelland photoacoustic cell, to ensure IR measurements under dry conditions. About 500 scans were taken with a resolution of 8 cm^{-1}. The PAS spectrometer was placed in an isolated bench, which was constantly purged with nitrogen to ensure that the samples were completely dried.

Transmission spectra were measured on a Nicolet20SX spectrometer equipped with a vacuum system cell and a DTGS detector and using a home-built in-situ vacuum IR transmission cell. Self-supporting disks with a thickness of 20 mg/cm^2 were used. One hundred scans were measured with a spectral resolution of 4 cm^{-1}.

Fourier transform Raman (FT-Raman) spectra were recorded on a Nicolet Nexus FT-Raman spectrometer with a Ge detector. All samples were measured at room temperature in a 180 °C reflective sampling configuration, with a 1064 nm Nd:YAG excitation laser. Five thousand scans were averaged for each spectrum and the laser power was set between 1 and 2.5 W.

Thermogravimetric (TG) measurements were performed on a Mettler TG50 thermobalance, equipped with a M3 microbalance and connected to a TC10A processor. Samples were heated from 30 °C to 50 °C and from 50 °C to 550 °C at a rate of 5 °C/min.

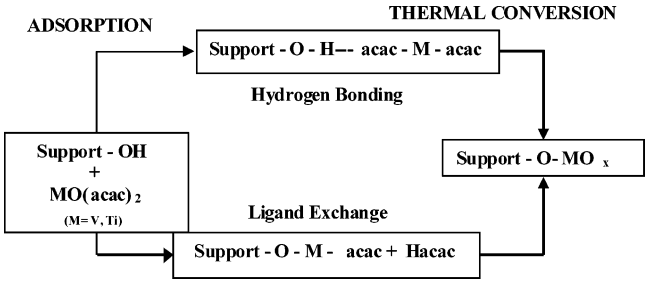

Figure 1. Schematic representation of the "molecular designed dispersion" method of acetylacetonates.

X-ray diffraction (XRD) patterns were collected on a Philips PW1840 powder diffractometer using Ni-filtered CuKα-radiation ($\lambda = 1.542$ Å)

Porosity and surface area studies were performed on a Quantachrome Autosorb 1 MP instrument. N_2 adsorption−desorption isotherms were recorded at 77K. The Brunauer−Emmett−Teller (BET) model was used to calculate the specific surface area. The pore diameter was calculated using the Barret−Joyner−Halenda (BJH) method. Micropore volume was calculated by the t-plot analysis and the total pore volume was calculated by means of the total amount of adsorbed gas at $P/P_o = 0.98$. The samples were outgassed overnight at room temperature for the precursors or at 200 °C for the supported oxides.

Results and Discussion

1. Characterization of the Precursors. 1.1. Single Depositions. Only results obtained from the single depositions, which will be useful for the understanding of the mixed oxide depositions, will be reported here.

The $TiO(acac)_2$ and $VO(acac)_2$ complexes acetylacetonate were grafted on the surface of the SBA-15 following the MDD method (Figure 1). A schematic representation of this MDD technique is depicted in Figure 1.

The adsorption of the complexes follows two different ways. One is by hydrogen bonding between an acetylacetonate ligand and the surface hydroxyls and the other one is by ligand exchange mechanism in which a covalent metal−oxygen support bonding is formed while an acetylacetonate ligand (Hacac) is lost. The calculation of *R*-value allows us to elucidate the reaction mechanism, since it reproduces the number of acac ligands associated with one metal (vanadium or titanium) atom.[6]

$$R = \frac{\text{mmol (acac)/gtotal}}{\text{mmol (Ti or V)/gtotal}}$$

Ligand exchange will result in an *R*-value of 1 as only one acetylacetonate ligand stays with the metal atom. Exclusive hydrogen bonding gives an *R*-value of 2 since there is no loss of any of the acac ligands. The concentration of the acac ligands on the silica surface was determined from the respective thermograms under oxygen atmosphere.

According to this MDD method, the surface of SBA-15 was modified with different amounts of Ti and also with V, using titanyl acetylacetonate and vanadyl acetylacetonate as the Ti and V sources, respectively. Figure 2 shows different initial concentrations of $TiO(acac)_2$ and $VO(acac)_2$ versus the final loading after reaction with the SBA-15 surface hydroxyls (OH concentration on the SBA-15 support is around 0.9−1 OH/nm^2).[20] When increasing the concentration of Ti and V, the final loading also increases until maximum coverage in which the range would keep constant.

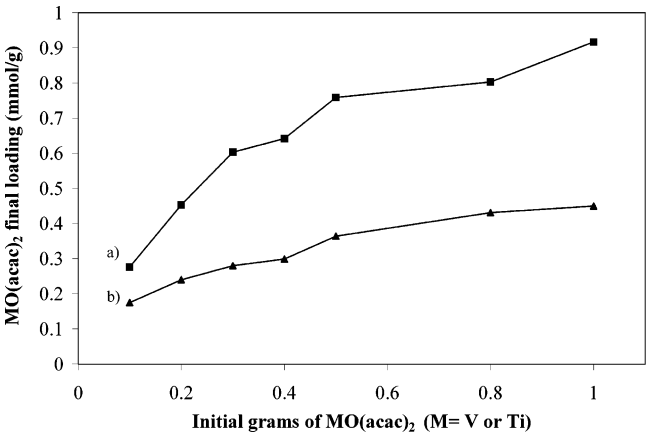

Figure 2. Initial grams of $TiO(acac)_2$ (a) and $VO(acac)_2$ (b) as a function of final loading (mmol/g) deposited on the SBA-15 support.

From these curves, it can be deduced that to cover around 50% of the OH of the SBA-15, ~0.76 mmol/g of Ti is necessary to deposit on the SBA-15 surface. In the case of vanadium, ~2.26 mmol/g of V are necessary to cover the remainder 50% of the OH of the SBA-15. From these data, we can conclude that titanium is more reactive toward the surface of the SBA-15 than vanadium.

Although Ti is more reactive than V, the adsorption of the complexes in both cases is mostly via hydrogen bonding with the hydroxyls of the support, since for all samples the *R*-value lies around 2. Also for reactions between the complexes and related silica supports, such as MCM-48, *R*-values of 2 are found.[17,21]

In Situ Transmission IR Spectroscopy. The decomposition of the anchored complexes on the SBA support and the conversion of the physisorbed species toward covalently bonded VO_x–TiO_x surface groups were studied by using a home-built in-situ vacuum IR transmission cell (Figure 3).

Transmission IR seems to be the only appropriate spectroscopic technique to follow the calcination process in working conditions, a process which is required to understand the reaction mechanism.

The samples were first analyzed by in-situ diffuse reflectance infrared Fourier transform (drift) spectroscopy but because of problems with water, the spectra were not well resolved. Moreover, the in-situ transmission cell solves the drawbacks of the commercial in-situ drift spectroscopy technique. The temperature can be totally controlled, as we use a calibrated oven instead of a digital one. The cell is connected to a volumetric apparatus supplied with diffusion and rotation pumps for its completely high vacuum condition. There are no problems arising from complex deposited on the mirrors, as the heating and measuring procedures are located in different zones and also the valve is closed during the heating time.

The detailed study of the single decomposition behavior of the single complexes on the SBA-15 surface by in-situ transmission IR, as presented in figure 4A and B, allows us to elucidate the reaction mechanism for the mixed oxide catalysts further on.

The interesting region to evaluate is between 1600 and 1400 cm^{-1}.[22] $TiO(acac)_2$ has a minor absorption at 1440 cm^{-1} and stronger bands at 1580 and 1530 cm^{-1}, whereas $VO(acac)_2$ shows absorptions at 1660, 1560, and 1530 cm^{-1} (Figure 4A and 4B). These bands assigned to V-acac disappear at 200 °C. However, $TiO(acac)_2$ spectra show the bands of acetylacetonate decreasing in intensity only at 300 °C. From these

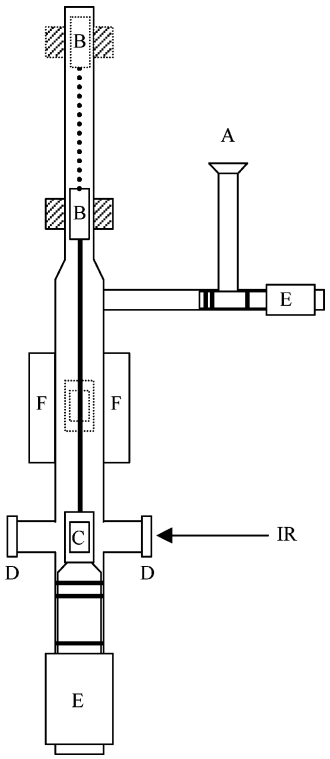

Figure 3. View of vacuum IR transmission cell. (A) Connection to volumetric apparatus, (B) bar magnet, (C) sample holder, (D) KBr window, (E) valves, (F) heating and reaction zone.

data, it can be concluded that $TiO(acac)_2$ has a higher thermal stability compared to $VO(acac)_2$.

1.2. Mixed Oxide Depositions. The synthesis parameters were optimized to obtain the final mixed oxide catalysts:

- Order of deposition: Titania was deposited first as it is usually used as a support and because the interaction silica−V is known to be weak.
- Concentration of the complexes: initial concentrations were calculated on the basis of obtaining a monolayer on the surface of the SBA-15.

Mixed oxide depositions were carried out calculating the concentration of Ti needed to react with 50% of the OH of the SBA-15 and calculating the concentration of V to react with the other 50% of the OH remaining on the SBA-15 surface. The mixed oxide depositions were carried out in a very controlled way to achieve a dispersed layer on the SBA-15 surface.

The Reaction Mechanism of $VO(acac)_2$–$TiO(acac)_2$ on SBA-15 Support. *A. Route A Deposition.* In route A deposition, $TiO(acac)_2$ was first deposited on the SBA-15 supported material. After removing the organic ligands by calcination, $VO(acac)_2$ complex was deposited on the TiO_x/SBA-15 surface.

Table 1 shows the final loading and *R*-value for the route A deposition which is compared to the results of the route B depositions.

Titanium shows much higher reactivity with SBA-15 than vanadium. The amount of Ti does not change after depositing vanadium and calcination of the precursor. Chemical analysis also shows that the final loading of Ti is the same by route B than by route A deposition. The final concentration of V deposited by route A is double than in route B deposition. However, the initial concentration of V used in route A and B were in both cases the same. This means that in the route A procedure, V centers are able to react with both the OH of the silica material and the Ti centers that are free of acac ligands

TABLE 1: Initial Concentration and Final Loading of V and Ti from Route A and Route B Deposition on SBA-15 Support[a]

	initial concentration		final loading		
sample	mmol V	mmol Ti	mmol/g V	mmol/g Ti	*R*-value
		route A			
SBA15−TiO_x−Vacac(prec)	2.26	0.76			(1.8)
SBA15−TiO_x−VO_x(calc)			0.25	0.55	2.6
		route B			
SBA15−Tiaca c−Vacac(prec)	2.26	0.76			
SBA15−TiO_x−VO_x (calc)			0.12	0.52	1.5

[a] Experiments were repeated eight times and a high reproducibility was obtained for all these samples. Average values are given in the table. The *R*-value between brackets was calculated from the single Ti deposition.

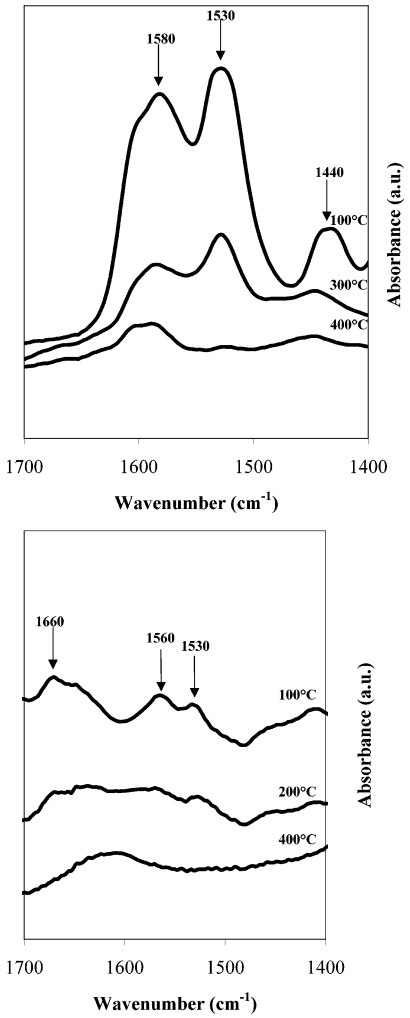

Figure 4. Thermal conversion process of single deposition $TiO(acac)_2$ (A) and $VO(acac)_2$ (B) on SBA-15, recorded in a vacuum as a function of temperature.

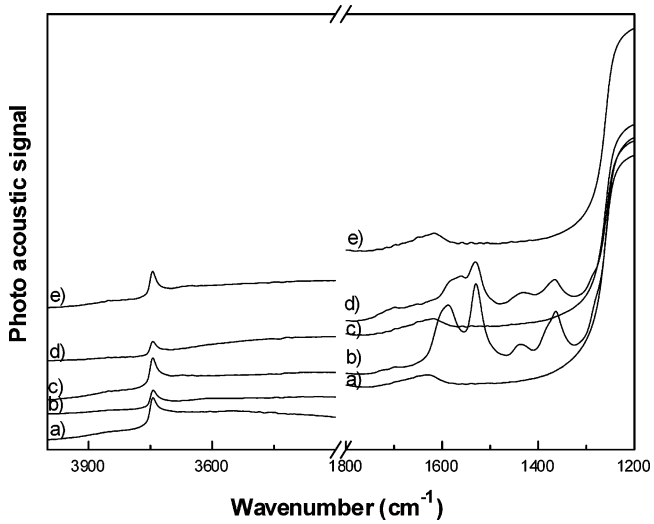

Figure 5. FTIR−PAS spectra of calcined SBA-15 (a), Ti-acac/SBA-15 precursor (b), TiO_x/SBA-15 calcined (c), V-acac/TiO_x/SBA-15 precursor (d), and final catalyst VO_x-TiO_x/SBA-15 (e).

after calcination. Further evidence of the reaction with the silica surface hydroxyls is given by FTIR−PAS, which shows a slight decrease of the silanol band after deposition of vanadium on TiO_x/SBA-15.

Figure 5 shows the FTIR−PAS spectra of blank SBA-15 thermally treated at 550 °C (Figure 5a), precursors (b, d), and final single catalyst (c) and final mixed oxide (e).

The spectra of the precursors show the characteristic acac vibrations of $TiO(acac)_2$ and $VO(acac)_2$ (spectra b and d, respectively) in the region 1600−1300 cm^{-1}. Decrease in the loading of the acac species can be assessed from the lowering of the intensity of the acac bands (spectra b, d)

Spectrum a shows a narrow band at 3745 cm^{-1}, assigned to isolated silanol groups, and a broad shoulder at around 3600 cm^{-1}, attributed to some bridged silanol groups. After the deposition of Ti (b) and V (d), a clear decrease in the intensity of the isolated silanol band at 3745 cm^{-1} is observed, although in both cases this band does not disappear. After calcination (spectra c and e), the silanol bands reappear with the formation of the final mixed oxide catalyst Si−O−Ti−O_x−V−O_x (spectrum e).

To elucidate the reaction mechanism, *R*-values are calculated. The *R*-value is always higher than 2 (average of 2.6 in Table 1), which theoretically is not possible as there is only one metal atom for two acac ligands. The only way to explain an *R* value higher than 2 is that there is a loss of vanadium centers. Therefore, we suggest the following hypothesis, confirmed by in-situ transmission IR, which explains the value of *R*.

In route A deposition, only V-acac bands are expected as the Ti is in the form of TiO_x. However, Figure 6 shows bands at 1660, 1580, 1530, and 1440 cm^{-1}. As it is shown in Figure 4A in the single V deposition, the band at 1660 cm^{-1} is indicative of the presence of some V-acac surface species, disappearing at 200 °C.

On the other hand, Figure 6 spectrum b shows bands at 1580, 1530, and 1440 cm^{-1} still at 300 °C and not disappearing at 200 °C as in the case of V-acac. This spectrum has the same pattern as the spectrum of Ti-acac species (Figure 4B), confirming that most of the acac species are present on the SBA-15 surface as Ti-acac. Between 200 and 300 °C, the Ti-acac bands are gradually disappearing proving that part of the acac ligands moved to the Ti centers. At 400 °C, all the organics are removed, yielding the final catalyst TiO_x-VO_x/SBA-15.

By in-situ transmission IR, it is clear that part of the acac ligands migrate to the Ti centers. As a result, some vanadium

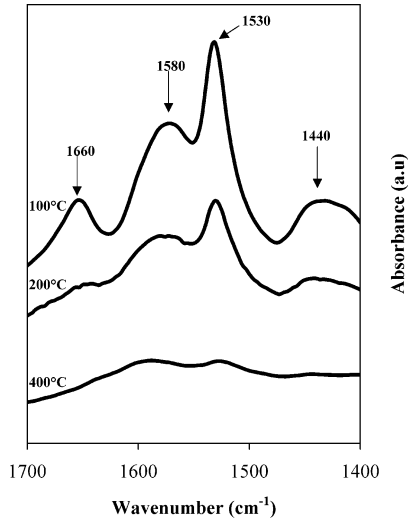

Figure 6. Thermal conversion process of a route A deposition (TiO_x−Vacac/SBA-15) as function of temperature.

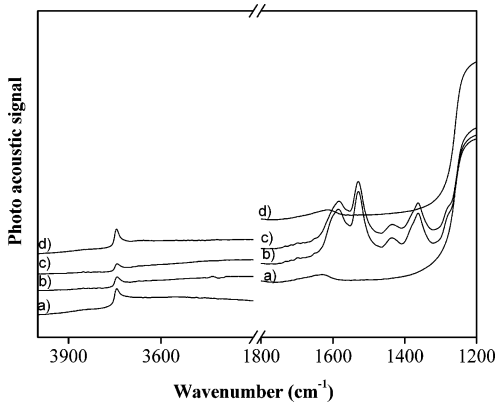

Figure 7. FTIR−PAS spectra of calcined SBA-15 (a), Ti-acac/SBA-15 precursor (b), V-acac/Ti-acac/SBA-15 precursor (c), and final catalyst VO_x−TiO_x/SBA-15 (d).

is lost during the washing off in the liquid deposition. Likewise, parts of the acac ligands remain on the sample migrating to the Ti centers. An additional proof to support the above hypothesis is the color of the toluene washing solution, turning green because of the presence of V.

B. Route B Deposition. In route B deposition, $VO(acac)_2$ is deposited on a noncalcined $TiO(acac)_2$/SBA-15 support.

R-value lies around an average of 1.5 (Table 1). The complexes are adsorbed via hydrogen bonding with the surface, although some part of the complexes is adsorbed via ligand exchange.

The final loading of the vanadium deposited on the surface is half of the loading deposited by route A deposition. In this case, the acac ligands from the V complex cannot move to the Ti as it is still surrounded by its own acac-ligands. As a result, V-centers can only react with the OH groups of the SBA-15. Anyhow, as already discussed above, the Ti loading and therefore its reactivity are much higher than vanadium.

Figure 7 shows the FTIR-pas spectra of blank SBA-15 thermally treated at 550 °C (Figure 7a), precursors (b, c), and final catalyst (d).

The spectra of the precursors show the characteristic acac vibrations in the region 1600−1300 cm^{-1}. After the deposition of Ti (b), a clear decrease of the isolated silanol band at 3745 cm^{-1} is observed and again a second decrease after deposition of V-acac (c). After calcination (d), the silanol band reappears

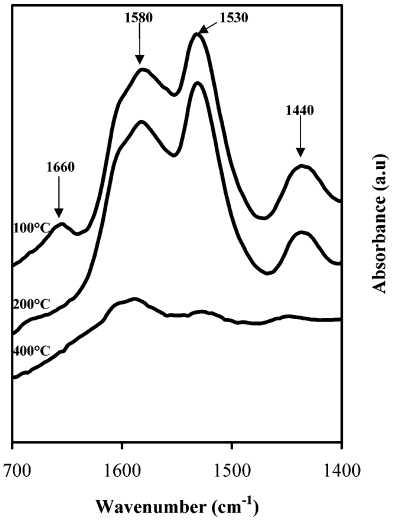

Figure 8. Thermal conversion process of a route B deposition (Tiacac−Vacac/SBA-15) as function of temperature.

with the formation of the final catalyst mixed oxide: Si−O−Ti−Ox−V−Ox (spectrum d).

In-situ transmission IR spectra show bands corresponding to a combination of V- and Ti-acac (Figure 8). At 200 °C, only the band at 1660 cm^{-1} assigned to V-acac disappeared and also bands at 1440 cm^{-1} and at 1580 cm^{-1} decrease in intensity. At 400 °C, all organics are removed.

2. Characterization of the TiO_x−VO_x Supported Mixed Oxides. Calcination of the precursor at 550 °C in ambient air removes the ligands and yields the final TiO_x−VO_x supported mixed oxide catalyst. Figures 5e and 7d show the infrared spectra of TiO_x−VO_x mixed oxides. All acac vibration modes have disappeared while the band of free silanols of the SBA-15 is partly restored. The same bands are observed for the final catalysts from both depositions.

FT-Raman Spectroscopy. Further information on the structure of the grafted support is given by FT-Raman spectroscopy. However, noncalcined samples were very difficult to measure as the color gave fluorescence and very easily, a broad heating band appears. The laser power then was decreased but this turns into a very weak signal and in some cases, the sample was already calcined.

After calcination, no such problem is faced; Raman spectroscopy is then a very interesting characterization tool as it is very sensitive to the presence of crystals, even if in XRD, TiO_2, or V_2O_5 crystallites are not seen, Raman would give typical bands of these crystals.

Raman spectra of calcined TiO_x−VO_x/SBA-15 obtained by route A and route B depositions show bands at 650, 520, 400, and 150 cm^{-1} (not shown). These are typical bands of anatase clusters attributed to anatase crystals TiO_2. As these signals are very strong, there are no signals of vanadium.

XRD and N_2-Adsorption. To study the structural changes of the SBA-15 after grafting with the acac complexes, XRD patterns and N_2-adsorption isotherms were recorded.

Figure 9 shows the XRD diffractograms of a blank SBA-15 and the same SBA-15 after adsorption of acetylacetonate complexes and its subsequent calcination.

The XRD pattern of the mixed oxide SBA-15 catalyst (both from routes B and A depositions) is very similar to the XRD of the calcined SBA-15 exhibiting one strong reflection (100) at $2\theta \sim 1$ and two weaker peaks (110) (200) at higher 2θ, associated with hexagonal symmetry and likewise characteristic of the hexagonally ordered structure of SBA-15.

TABLE 2: Structural Properties of Blanks, Precursors, and Final Mixed Oxide Catalysts on SBA-15 Support

sample	^{SBET} (m^2/g)	mesopore vol. (cc/g)	micropore vol. (cc/g)	pore radius (Å)	total pore volume (cc/g)
			route A		
SBA15 blank	744	0.75	0.101	25.40	0.85
SBA15−TiO_x	582	0.52	0.099	32.54	0.62
SBA15−TiO_x −VO_x	492	0.49	0.071	25.55	0.56
			route B		
SBA15 blank	640	0.57	0.105	32.56	0.68
SBA15−Tiaca−Vacac	401	0.36	0.043	25.07	0.40
SBA15−TiO_x−VO_x	525	0.49	0.055	30.81	0.54

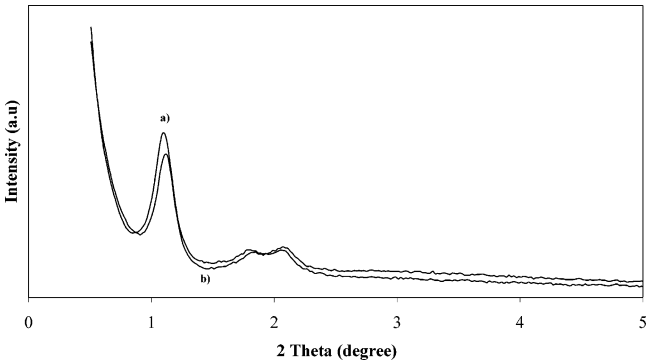

Figure 9. XRD patterns of blank SBA-15 (a) and TiO_x-VO_x/SBA-15 (b).

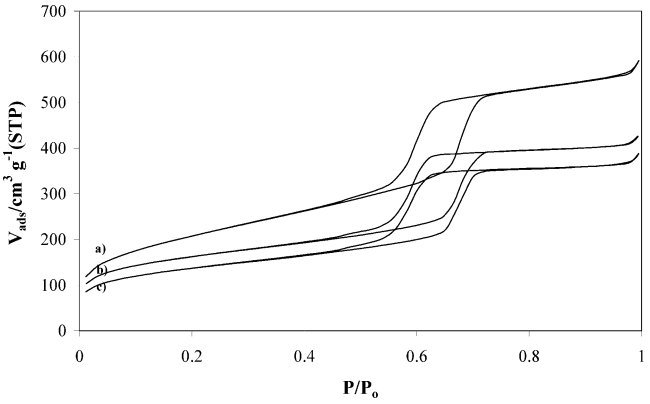

Figure 10. Nitrogen adsorption−desorption isotherms for a mixed oxide sample obtained by route A deposition. Pure SBA-15 (A), TiO_x/SBA-15 (B), and mixed oxide TiO_x-VO_x/SBA-15 (C).

Very similar diffraction peaks are observed for pure SBA-15 and the final catalyst, although the intensity of the peaks is slightly reduced. It means that the crystallinity and the ordering of the SBA-15 are retained after modification of the surface, independently of the way of depositing both metals.

The estimated structural parameters such as specific surface area, S_{BET}, BJH pore radius, and mesopore and micropore volume, for the two types of synthesized samples are summarized in Table 2.

The calculated BET surface area for the calcined support material is between 600 and 800 m^2/g, which decreases with increasing metal loading. The pores of the SBA-15 support are filled by grafting the surface OH groups with the metal acac complexes. As a result, the porosity and surface area are reduced.

After calcination of the precursor, the metal complexes are converted into the V−Ti mixed oxides. Consequently, the pores are released, the pore volume is restored to about 70−80% of the original value, and the surface area and porosity increase again.

Figures 10 and 11 show nitrogen adsorption/desorption isotherms for the blank SBA-15 and samples obtained by route A and route B depositions, respectively.

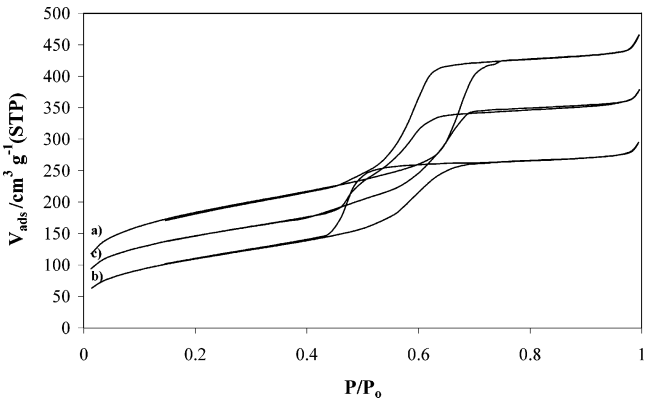

Figure 11. Nitrogen adsorption−desorption isotherms for a mixed oxide sample obtained by route B deposition. Pure SBA-15 (A), precursor Tiacac−Vacac/SBA-15 (B) and mixed oxide TiO_x-VO_x/SBA-15 (C).

All adsorption/desorption isotherms are Type IV according to IUPAC classification and exhibit a H1 hysteresis loop, which is typical for mesoporous materials.[23]

The isotherms of the calcined SBA-15 and the grafted materials exhibit a sharp increase in the adsorbed N_2 volume at $P/P_0 \sim 0.7$, characteristic of capillary condensation within the uniform mesopores of the materials.

As evidenced by these N_2 adsorption−desorption isotherms, route A and B depositions end up with differences in pore structure for the final catalysts, because of the way of preparation.

TiO_x-VO_x/SBA-15 catalyst obtained by route A deposition exhibits isotherms shown in Figure 10. Adsorption and desorption both exhibit one-step branch. During the desorption process, the pores begin to empty at a pressure related to the meniscus of liquid N_2 in the pores. All pores empty at approximately the same pressure, leading to a one-step desorption branch.

TiO_x-VO_x/SBA-15 catalyst obtained by route B deposition exhibits isotherms shown in Figure 11. The shape of the hysteresis changes for the blank SBA-15, precursor, and final catalyst. The precursor shows an ink-bottle type of hysteresis, which indicates the presence of pores that are very narrow at the entrances. This will be the result of the metal particles inside the channels of SBA-15 as the bulky acac-ligands are still present causing the wide hysteresis.

When the isotherms corresponding to the blank SBA-15 and the final catalysts are compared, a significant difference can be noticed. In the isotherm of the final catalyst, the adsorption occurs in one step but there are two desorption steps (second step at the relative pressure of ca. 0.5) indicating a pore blocking effect. This adsorption−desorption behavior agrees with the structure comprising both open and closed cylindrical mesopores, because of the formation of metal oxide plugs in the SBA-15 channels.

The open mesopores (close to the pore entrances) empty during the desorption according to the normal Kelvin model;

however, the closed mesopores, which are situated in the SBA-15 channels between the plugs, have diffusion limitations in the nitrogen adsorption isotherm causing the lower-pressure plateau in the desorption branch.[25] This means that route B deposition induces the blocking of the pores of the SBA-15 because of the way the metals are deposited on the SBA-15.

As the total concentration of the mixed oxide is comparable to the Ti concentration in a single deposition while in the latter case no pore blocking is noticed, it can be concluded that the pore blocking only occurs when V oxide is present and when they are deposited by route B. Pore blocking also depends on the order of the metals in the deposition process as the pore blocking only occurs when V-acac is deposited after Ti-acac.

These results support the idea of a different distribution of the metals according to the way of deposition. In route A deposition, the Ti complex is first calcined and spread out along the tubes of the SBA-15 material; after calcination, vanadium acac is deposited. Vanadium centers are able to react with the OH of the SBA-15 as well as with with TiO_x, so in this case the double of V is deposited compared to route B deposition. Upon calcination, vanadium is spread out, mainly over the titanium layer inside the tubes of the support. This leads to an open pore structure for the SBA-15 catalyst, as proven by N_2 adsorption−desorption. However, mixed oxides deposited by route B show plugs of the metal oxides. The structure is a combination of open and blocked cylindrical mesopores.

In this case, Ti-acac complex is deposited first, not followed by calcination, and bulky vanadium complex is deposited afterward. Ti blocks the entrance of the pores because it is not calcined and the acac ligands remain at the Ti centers. In this case, V-acac reacts only with the OH of the SBA-15 and they remain at the pore entrance, forming the plugs after calcination.

Conclusion

TiO_x−VO_x mixed oxides supported SBA-15 catalysts were prepared in a controlled way. SBA-15 is used as a support on the basis of its interesting characteristics such as high porosity, high pore volumes, thick pore walls, and a combination of micro- and mesopores. The Ti and V active centers on SBA-15 support are generated by the MDD method of the $TiO(acac)_2$ and $VO(acac)_2$. The decomposition of the anchored complexes on the SBA-15 support toward covalently bonded TiO_x −VO_x surface groups were studied by using an in-situ IR transmission cell.

Route A and route B depositions of both metals are presented to prepare mixed oxides catalysts in a very controlled way. In both cases, the V interaction is weak, and titanium is much more reactive with the silica surface than vanadium.

In route A deposition, a detailed IR study was performed to establish that Ti-acac species are formed because of the migration of the acac ligands from the V centers to the Ti centers, while at the same time V is lost in the washing step as a part of the deposition process. Also, the vanadium concentration deposited on the final catalyst is double than the one obtained in route B deposition. This is due to the fact that vanadium is able to react with both the OH from the silica as well as with the Ti centers.

In route B deposition, the final loading of Ti is the same as in route A deposition, but the V concentration is lower because V-acac only reacts with the OH of the silica, as evidenced in both depositions by IR spectroscopy.

Depending on the way of preparation of the mixed oxides, the final catalysts present differences in the pore structure, showing partially blocked pores when deposited by route B, because of the formation of metal oxide plugs in the pore channels of the SBA-15. However, in both ways of deposition, porosity and crystallinity of the final catalyst is still high.

The catalytic properties of these materials will be reported in a future paper.

Acknowledgment. P. Cool and V. Meynen acknowledge the FWO-Flanders (Fund for Scientific Research-Flanders) for financial support.

References and Notes

(1) Corma, A. *Chem. Rev.* **1997**, *97*, 2373−2419.
(2) Soler-Illia G. J. de A. A.; Sanchez, C.; Lebeau, B.; Patarin, J. *Chem. Rev.* **2002**, *102*, 4093−4138.
(3) . Lin, C−H.; Bai, H. *Appl. Catal., B* **2002**, *1306*, 1−9.
(4) Lietti, L.; Nova, I.; Ramis, G.; Dall'Acqua, L.; Busca, G.; Giamello, E.; Forzatti, P.; Bregani, F. *J. Catal.* **1999**, *187*, 419−435.
(5) Economidis, N. V.; Pena, D. A.; Smirniotis, P. G. *Appl. Catal., B* **1999**, *23*, 123−134.
(6) Baltes, M.; Collart, O.; Van Der Voort, P.; Vansant, E. F. *Langmuir* **1999**, *15*, 5841.
(7) Collart, O.; Van Der Voort, P.; Vansant, E. F.; Gustin, E.; Bouwen, A.; Schoemaker, D.; Ramachandra, R. R.; Weckhuysen, B. M.; Schoonheydt, R. A. *Phys. Chem. Chem. Phys.* **1999**, *1*, 4099.
(8) Van Der Voort, P.; Van Welzenis, R.; De Ridder, M.; Brongersma, H. H.; Baltes, M.; Mathieu, M.; Van de Ven, P. C.; Vansant, E. F. *Langmuir* **2002**, *18*, 4420−4425.
(9) Cool, P.; Van der Voort, P.; Vansant, E. F. *Encyclopedia of Surface and Colloid Science*; Hubbard, A., Ed.; Marcel Dekker Inc.: New York, 2002; pp 5244−5256.
(10) Handy, B. E.; Baiker, A.; Schraml-Marth, M.; Wokaun, A. *J. Catal.* **1992**, *133*, 1−20.
(11) Nova, L.; Dall'Acqua, L.; Lietti, L.; Giamello, E.; Forzatti, P. *Appl. Catal., B* **2001**, *35*, 31−42.
(12) Molina, R.; Centeno, M. A.; Poncelet, G. *J. Phys. Chem. B* **1999**, *103*, 6036−6046.
(13) Van der Voort, P.; White, M. G.; Vansant, E. F. *Langmuir 14*, **1998**.
(14) Baltes, M.; Van Der Voort, P.; Collart, O.; Vansant, E. F. *J. Porous Mater*. **1998**, *5*, 317.
(15) Baltes, M.; Van Der Voort, P.; Weckhuysen, B. M.; Rao, R. R.; Catana, G.; Schoonheydt, R. A.; Vansant, E. F. *Phys. Chem. Chem. Phys*. **2000**, *2*, 2673.
(16) Van Der Voort, P.; Baltes, M.; Vansant, E. F. *J. Phys. Chem. B* **1999**, 10102−10108.
(17) Schrijnemakers, K.; Vansant, E. F. *J. Porous Mater*. **2001**, *8*, 83.
(18) Zhao, D.; Huo, Q.; Feng, J.; Chmelka, B. F.; Stucky, G. D. *J. Am. Chem. Soc*. **1998**, *120*, 6024−6036.
(19) Vogel, Arthur I. *Quantitative Inorganic Analysis*, 3rd ed.; Longman: London, 1971; p 790.
(20) Vansant, E. F.; Van Der Voort, P.; Vrancken, K. C. Characterization and Chemical Modification of the Silica Surface. *Studies in Surface Science and Catalysis*; Elsevier: Amsterdam, 1995.
(21) Baltes, M.; Cassiers, K.; Van Der Voort, P.; Weckhuysen, B. M.; Schoonheydt, R. A.; Vansant, E. F. *J. Catal.* **2001**, *197*, 160−171.
(22) Lawson, E. K. *Spectrochim. Acta* **1961**, *17*, 248−258.
(23) De Boer, J. H.; Linsen, B. G.; Osinga T. J. *J. Catal.* **1964**, *4*, 643.
(24) Van Der Voort, P.; Ravikovitch, P.; Neimark, A. V.; Benjelloun, M.; Weckhuysen, B. M.; Vansant, E. F. *Stud. Surf. Sci. Catal.* **2002**, *141*, 45−52.